Inorganic Chemistry

Article

pubs.acs.org/IC

Solvated-Ion-Pairing-Sensitive Molecular Bistability Based on Copper(I)-Coordinated Pyrimidine Ring Rotation

Michihiro Nishikawa, Kuniharu Nomoto, Shoko Kume,*[,†] and Hiroshi Nishihara*

Department of Chemistry, School of Science, The University of Tokyo, 7-3-1 Hongo, Bunkyo-ku, Tokyo 113-0033, Japan

Supporting Information

ABSTRACT: We describe herein the effect of solvated ion pairing on the molecular motion of a pyrimidine ring coordinated on a copper center. We synthesized a series of heteroleptic copper(I) complex salts bearing an unsymmetrically substituted pyridylpyrimidine and a bulky diphosphine. Two rotational isomers of the complexes were found to coexist and interconvert in solution via intramolecular ligating atom exchange of the pyrimidine ring, where the notation of the inner (i-) and outer (o-) isomers describes the orientation of the pyrimidine ring relative to the copper center. The stability of the pyrimidine orientation was solvent- and counterion-sensitive in both **2**·BF_4 {$\mathbf{2}^+$ = [Cu(Mepypm)(dppp)]$^+$, where Mepypm = 4-methyl-2-(2′-pyridyl)pyrimidine and dppp = 1,3-bis(diphenylphosphino)propane} and previously reported **1**·BF_4, which possesses a bulky diphosphine ligand ($\mathbf{1}^+$ = [Cu(Mepypm)(DPEphos)]$^+$, where DPEphos = bis[2-(diphenylphosphino)phenyl] ether). Two rotational isomers of $\mathbf{2}^+$ were separately obtained as single crystals, and the structure of each isomer was examined in detail. Both the enthalpy and entropy values for the rotation of **2**·BF_4 in $CDCl_3$ (ΔH = 6 kJ mol^{-1}; ΔS = 25 J K^{-1} mol^{-1}) were more positive than that tested under other conditions, such as in more polar solvents CD_2Cl_2, acetone-d_6, and CD_3CN. The reduced contact of the anion to the cation in a polar solvent seems to contribute to the enthalpy, entropy, and Gibbs free energy for rotational isomerization. This speculation based on solvated ion pairing was further confirmed by considering the rotational behavior of $\mathbf{2}^+$ with a bulky counterion, such as $B(C_6F_5)_4^-$. The findings are valuable for the design of molecular mechanical units that can be readily tuned via weak electrostatic interactions.

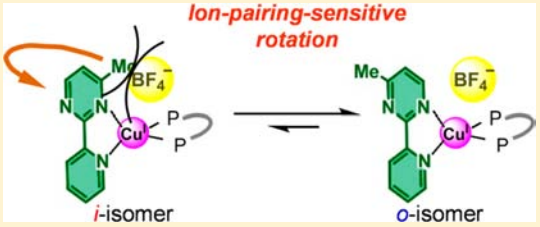

INTRODUCTION

Solvated ion pairing is valid for both traditional and recent topics of chemistry, such as electron transfer,[1−3] general reactions,[4,5] charge separation,[6] molecular machines,[7−12] ion sensing,[13−15] and ionic liquids.[16] An ion pair consists of an equilibrium between several different states that include the anion and cation present as a solvated contact ion pair (CIP), a solvent-shared ion pair, a solvent-separated ion pair (SSIP), and unpaired solvated ions.[17] Because ion pairing between the metal complex cation and counteranion has often been found to play a key role in the functionalization of molecular systems, detailed studies on the solvation are valid for the development of promising materials.[18−30] In the present study, we investigated ion-pair effects on a metal complex bistability caused by intramolecular ligating atom exchange using simple heteroleptic copper(I) complexes bearing an unsymmetrically substituted pyridylpyrimidine and a bulky diphosphine ligand.

The copper(I) state prefers to adopt a tetrahedral geometry because of its d^{10} electronic configuration.[26−52] The bidentate diimines on copper(I) undergo ligand-substitution reactions at slow rates under ambient temperatures.[28−32] In addition, the labile Cu−N bond rearrangement is valid for applications in nanoscience.[20−22,33−35] Furthermore, the photophysics of simple heteroleptic copper(I) complexes bearing a diimine and a diphosphine ligand has attracted significant attention not only for fundamental studies pertaining to their intense luminescence[36−48] but also for use in applications.[39−42] A family of [Cu(diimine)(DPEphos)]$^+$ (DPEphos = bis[2-(diphenylphosphino)phenyl] ether) complexes has been particularly well studied owing to their intense luminescence.[43−46] The luminescence of [Cu(diimine)(dppp)]$^+$ [dppp = 1,3-bis(diphenylphosphino)propane] derivatives has also been examined in detail.[47]

We introduced a bidentate ligand consisting of a coordinated pyrimidine moiety that could effectively alternate between two possible coordination geometries at the copper center via rotational isomerization.[53−59] The ring rotation has been exploited for modulation of the electrode potential of [Cu(Mepypm)(L_{anth})]BF_4 [Mepypm = 4-methyl-2-(2′-pyridyl)pyrimidine; L_{anth} = 2,9-bis(9-anthryl)-1,10-phenanthroline],[53] for the manipulation of intramolecular electron transfer,[54] for the development of a redox potential switch based on photodriven rotation,[58] and in the demonstration of the dual-luminescence behavior of [Cu(Mepypm)(DPEphos)]-BF_4 (**1**·BF_4),[57] considering well-established copper(II/I) redox properties.[20−22,33−35,60−63] We have also reported that the equilibrium of **1**·BF_4 between the two rotational isomers in the copper(I) state depends significantly on both the solvent and temperature, as confirmed by analysis in chloroform-

Received: October 2, 2012
Published: December 13, 2012

$d_1(CDCl_3)$, acetone-d_6, and acetonitrile-d_3 (CD_3CN) at variable temperature.[57]

In the present paper, we investigate in detail the effect of ion pairing on the rotational dynamics of $[Cu(Mepypm)(dppp)]^+$ ($\mathbf{2}^+$). The coordination geometry of the diphosphine moiety differs from that previously described. Two kinds of noncoordinative counterions are considered,[64−67] BF_4^- and $B(C_6F_5)_4^-$, where the latter is much larger than the former. The chemical equilibrium of the isomers is illustrated in Figure 1, where the notation of the inner (i-) and outer (o-) isomers

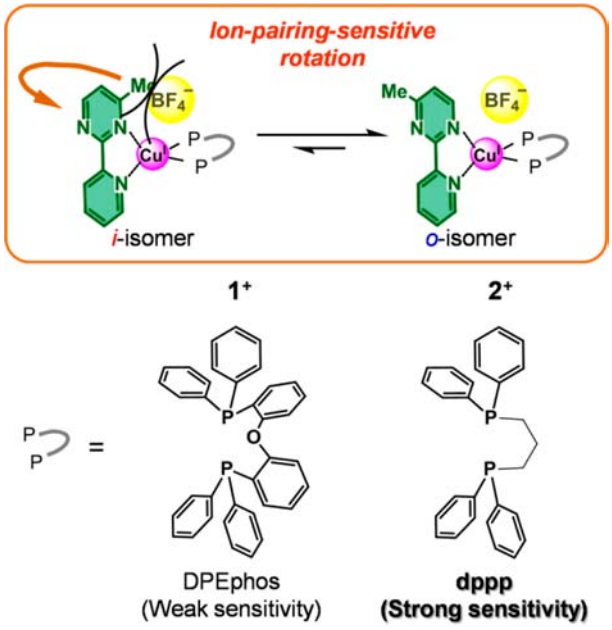

Figure 1. Conceptual diagram showing the effect of ion pairing on the chemical equilibrium of pyrimidine ring rotational isomerization.

describes the orientation of the pyrimidine ring. To elucidate the ion-pairing sensitivity, we describe the rotational equilibrium for both $\mathbf{1}\cdot BF_4$ and $\mathbf{1}\cdot B(C_6F_5)_4$. We found that the dynamics requires a consideration of the relationship between the solvated ion pairing and the pyrimidine ring rotation.

RESULTS AND DISCUSSION

Synthesis and Characterization of the Rotational Equilibrium in Solution. $\mathbf{1}\cdot B(C_6F_5)_4$, $\mathbf{2}\cdot BF_4$, and $\mathbf{2}\cdot B(C_6F_5)_4$ were synthesized using a modified literature method (Scheme 1).[44,47,57] In this approach, tetrakis(acetonitrile)copper(I) salt was reacted with a diphosphine ligand and a Mepypm ligand in dichloromethane at room temperature. The obtained compounds were characterized by ^1H NMR and elemental analysis.

Scheme 1. Synthesis of $\mathbf{2}\cdot BF_4$ and Reference [Cu(diimine)(diphosphine)]X Complexes

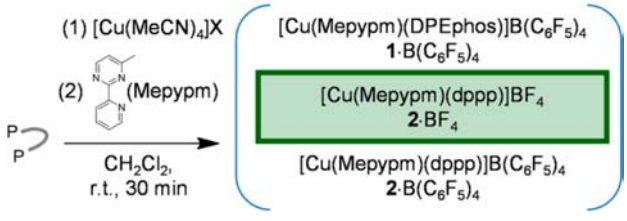

The rotational bistability of $\mathbf{2}\cdot BF_4$ in $CDCl_3$, dichloromethane-d_2 (CD_2Cl_2), acetone-d_6, acetonitrile-d_3 (CD_3CN), $\mathbf{2}\cdot B(C_6F_5)_4$ in $CDCl_3$, $\mathbf{1}\cdot BF_4$ in $CDCl_3$, CD_2Cl_2, acetone-d_6, and CD_3CN, and $\mathbf{1}\cdot B(C_6F_5)_4$ in $CDCl_3$ was characterized using ^1H NMR analysis to monitor chemical exchange (Figure 2 and the

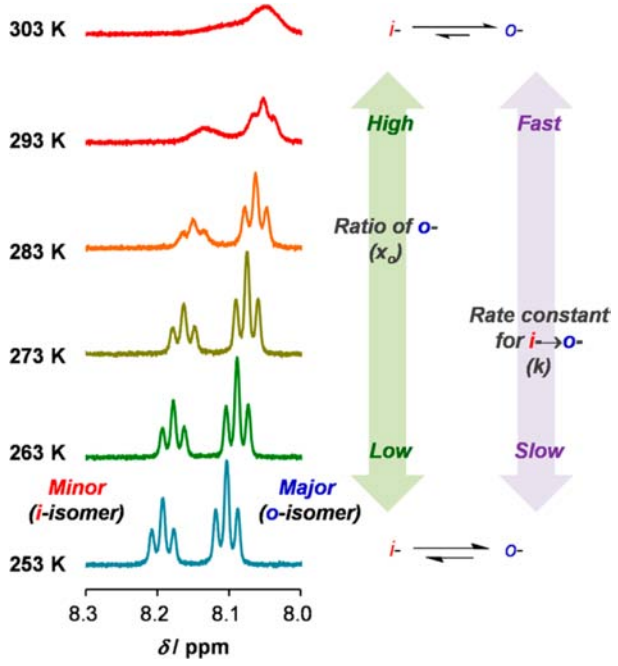

Figure 2. Aromatic ^1H NMR signal of a Mepypm moiety in $\mathbf{2}\cdot BF_4$ in $CDCl_3$ at several temperatures. The signals derived from i- and o-isomers are represented as red and blue, respectively. Illustration of the ratios and the rate of the rotational equilibrium are also described on the right side.

Supporting Information, Figures S1−S10). Integration of ^1H NMR spectra along with line-shape analysis are well-established methods[68,69] for investigating the thermodynamics and kinetics of a chemical equilibrium.[70−78] Two clearly resolved sets of signals were observed in the ^1H NMR spectrum of $\mathbf{2}\cdot BF_4$ in $CDCl_3$ at 253 K. Signal splitting was also observed in the aromatic proton signals of the Mepypm ligand (Figure 2). The ratio of o-isomers, estimated from integration of the minor and major signals, is represented as x_o %. The ratio of i-isomer is thus $(100 - x_o)$ %. Consider, for instance, that at 253 K the x_o value was determined to be 59%; the reason for higher x_o values at higher temperature is described in the later sections. Upon heating, these signals broadened, indicating that i- and o-isomers interconverted in solution on a time scale that is commensurate with that of the ^1H NMR measurement (Figure 2). The rate constant for the i → o isomerization, k, was estimated from simulated fittings of the broadened ^1H NMR spectra (Supporting Information, Figure S1b). For example, the value of k was 100 s^{-1} at 303 K; a faster rate of rotation at higher temperature is normal for chemical equilibrium. These parameters, at several temperatures and under various conditions, were determined by the same analysis as that described above.

The i/o ratios and their heat sensitivities, along with their isomerization rates, are dependent on the solvent and counterion (Supporting Information, Figures S1−S10). However, a complete description of the observed effects requires a

dx.doi.org/10.1021/ic302141z | Inorg. Chem. 2013, 52, 369−380

close consideration of the geometry of the complexes, as highlighted in later sections.

The interconversion between the two rotational isomers is generally an intramolecular process, as confirmed by ^{1}H NMR analysis of a mixed solution of **1**·BF_4 and [Cu(bpy)(DPEphos)]BF_4 (**3**·BF_4; bpy = 2,2′-bipyridine), which does not undergo rotation,[57] This strategy is based on a modified method described in the literature.[70b] The rate of interconversion between i- and o-isomers (k) via an intramolecular process is denoted as k_{intra}, which via an intermolecular process is k_{inter} ($k = k_{intra} + k_{inter}$). The value of k_{inter} is evaluated from the rate of interconversion between **3**·BF_4 and **1**·BF_4 because both processes require intermolecular diimine ligand exchange. A ^{1}H NMR spectrum of **3**·BF_4 in acetone-d_6 at room temperature displayed one set of signals derived from the diimine moiety (Figure 3, middle). Two sets of broadened signals derived from

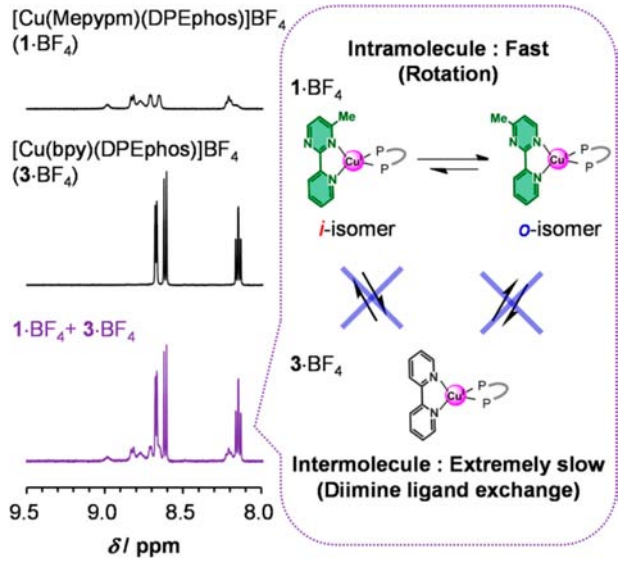

Figure 3. (left) Partial ^{1}H NMR spectra of **1**·BF_4 (top), **3**·BF_4 (middle), and a mixture of **1**·BF_4 and **3**·BF_4 (bottom) in acetone-d_6 in the dark at room temperature (right). Illustration of the interconversion between species in a mixed solution of **1**·BF_4 and **3**·BF_4.

i- and o-isomers were observed in a ^{1}H NMR spectrum of **1**·BF_4 under the same conditions (Figure 3, top). A ^{1}H NMR spectrum of a mixed solution of **3**·BF_4 and **1**·BF_4 under the same conditions was simply a superposition of the two spectra (Figure 3, bottom), suggesting that the intermolecular interconversion between **3**·BF_4 and **1**·BF_4 via a diimine ligand exchange reaction was extremely slow compared with the time scale of the ^{1}H NMR measurement (Figure 3, right). In addition, the ^{1}H NMR spectrum of the solution showed no signal broadening derived from **3**·BF_4 at 313 K (Supporting Information, Figure S11), where the estimated rate constant for interconversion between i- and o-isomers (k) was 300 s^{-1}. The rate constant for the intermolecular process under the given conditions (k_{inter}) was smaller than ca. 1 s^{-1} ($k \gg k_{inter}$). Therefore, interconversion between i- and o-isomers in typical organic solvents at ambient temperature is dominated by the intramolecular process ($k_{intra} \gg k_{inter}$). Possibilities of a faster intermolecular process ($k_{intra} \sim k_{inter}$ or $k_{intra} \ll k_{inter}$) can be denied from small differences in the signal broadness between three species derived from i- and o-isomers of **1**·BF_4 and **3**·BF_4.

This interpretation is supported by the fact that the shape of the peaks in the ^{1}H NMR spectrum of **1**·BF_4 in acetone-d_6 at room temperature displayed no dependence on the concentration (Supporting Information, Figure S12). The evidence of intramolecular rotational isomerization is valid to drive our previous rotational system[53−58] in the single molecular level.

Crystallography. We performed single-crystal X-ray structural analysis of **1**·$B(C_6F_5)_4$, **2**·BF_4, and **2**·$B(C_6F_5)_4$ (Figure 4 and the Supporting Information, Figures S13−S17

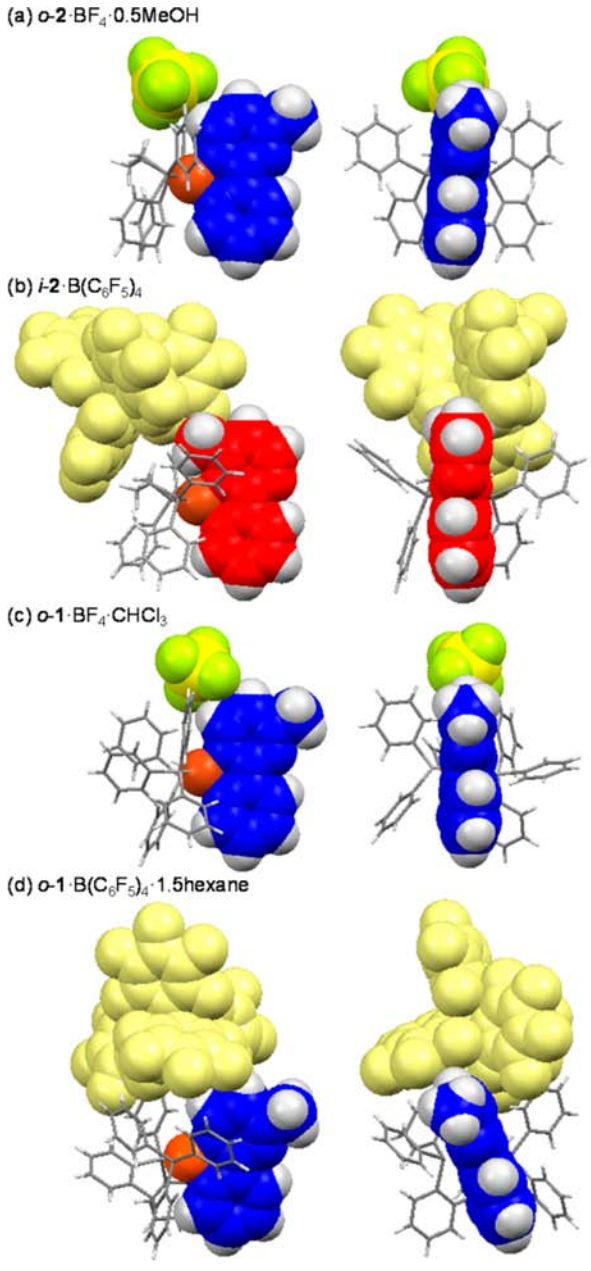

Figure 4. Side (left) and front (right) views of the crystal structures of o-**2**·BF_4·0.5MeOH (a), i-**2**·$B(C_6F_5)_4$ (b), o-**1**·BF_4·$CHCl_3$ (c), and o-**1**·$B(C_6F_5)_4$·1.5hexane (d). The carbon atoms in the Mepypm moiety are blue or red, which correspond to o- and i-isomers, respectively. The Mepypm moiety, copper atom, and counterion are drawn as a space-filling model, whereas the diphosphine moiety is included as a capped stick model. For clarity, some molecules are omitted: (a) a complex cation, a BF_4^- ion, and a methanol molecule; (c) a chloroform molecule; (d) hexane molecules.

dx.doi.org/10.1021/ic302141z | Inorg. Chem. 2013, 52, 369−380

and Table S1). The previously reported crystal structure of $1{\cdot}BF_4$[57] was also employed for comparison. The ratio of the complex cation to the counterion in the asymmetric unit was 1:1, suggesting that the oxidation state of the metal atom was copper(I) in the single crystal. The geometric parameters of the complex cations in $1{\cdot}BF_4$, $1{\cdot}B(C_6F_5)_4$, $2{\cdot}BF_4$, and $2{\cdot}B(C_6F_5)_4$ such as the bond lengths were in agreement with the ones of the family of $[Cu(diimine)(diphosphine)]^+$ complexes (Supporting Information, Table S2).[43−47] The methyl group of the Mepypm moiety in $2{\cdot}BF_4$ is oriented outward of the metal center, and no disorder was found in the coordination mode. This result suggests that all 2^+ species in the single crystal exist solely as the o-isomer, which corresponds to a pyrimidine moiety orientation that is identical with that of the previously reported crystal structure of $1{\cdot}BF_4$ (Figures 4a,c).[57] In contrast, the methyl group in $2{\cdot}B(C_6F_5)_4$ is directed toward the metal center, indicating that all 2^+ species exist as the i-isomer in the single crystal (Figure 4b). Furthermore, all 1^+ species in $1{\cdot}B(C_6F_5)_4$ exist as the o-isomer (Figure 4d), which is identical with $1{\cdot}BF_4$ from the viewpoint of pyrimidine orientation. On the basis of the orientation of pyrimidine in the crystal as well as considering the solvents to have negligible interaction with the complex cation, the four single crystals are denoted as o-$2{\cdot}BF_4{\cdot}0.5MeOH$, i-$2{\cdot}B(C_6F_5)_4$, o-$1{\cdot}BF_4{\cdot}CHCl_3$, and o-$1{\cdot}B(C_6F_5)_4{\cdot}1.5$hexane.

In the case of o-$1{\cdot}BF_4{\cdot}CHCl_3$, the copper center is surrounded by the coordinating nitrogen atoms, a bulky diphosphine moiety, and a BF_4^- ion. The interaction of the BF_4^- ion with the copper center in o-$2{\cdot}BF_4{\cdot}0.5MeOH$ is significantly stronger than that in o-$1{\cdot}BF_4{\cdot}CHCl_3$, considering the Cu−B distance. These results reflect the reduced bulkiness of dppp, owing to the presence of fewer phenyl groups, compared with DPEphos. In contrast, the methyl group in i-$2{\cdot}B(C_6F_5)_4$ is located nearer to the copper atom than the counteranion. $B(C_6F_5)_4^-$ is distant from the copper center because of a large steric repulsion between $B(C_6F_5)_4^-$ and the complex cation. Because of a coordination geometry similar to that of o-$2{\cdot}BF_4{\cdot}0.5MeOH$, the proximity of the counterion is seemingly the primary cause for destabilization in the i-isomer. On the other hand, the methyl group did not cover the copper center in $1{\cdot}B(C_6F_5)_4$, which is similar to o-$1{\cdot}BF_4{\cdot}CHCl_3$. The results suggest that the position of the counterion has a small effect on the orientation of pyrimidine in 1^+ most likely because of the bulkiness of the diphosphine moiety. As a result, the effects of the counterion on the rotational dynamics of 2^+ are expected to be more significant than those operative in 1^+. The aforementioned trend is characteristic of the $[Cu(Mepypm)(diphosphine)]^+$ family because of the geometry of the diphosphine ligand. Such behavior was not observed when bulky diimines were employed as the auxiliary ligand, such as in $[Cu(Mepypm)(L_{anth})]^+$.[53] Examination of the crystal packing in the presented complexes reveals that the proximity of other species, such as solvent molecules or another complex salt, was less than that of the nearest counterion described above (Supporting Information, Figures S14−S17). The obtained crystal structures enable us to effectively construct a reasonable model for the sensitivity of rotational equilibrium on a weak interaction in a solution state, which is described in the following section.

Results for the Thermodynamics of Rotation in Solution. The thermodynamics of the rotational equilibrium of $2{\cdot}BF_4$ and $2{\cdot}B(C_6F_5)_4$, along with the reference compounds $1{\cdot}BF_4$ and $1{\cdot}B(C_6F_5)_4$, was examined. The values of enthalpy (ΔH), entropy (ΔS), and Gibbs free energy (ΔG) for the i → o rotation were obtained using van't Hoff plots that were estimated from integration of the ^{1}H NMR spectra at various temperatures in different solvents (Figure 5). A negative ΔG corresponds to a predominance of the o-isomer compared with the i-isomer. A positive ΔH value corresponds to an enthalpic stabilization of the i-isomer and a positive ΔS value to an entropic stabilization of the o-isomer. The significant heat sensitivity of the isomer ratios (Figure 2) indicated the large value of ΔH. We denote ΔG and x_o at 298 K as ΔG_{298} and $x_{o,298}$, respectively. Selected parameters are tabulated in Table 1 and the Supporting Information, Table S3.

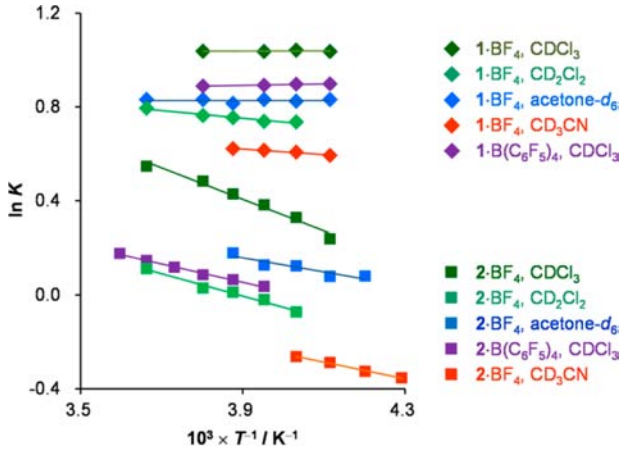

Figure 5. van't Hoff plots for the rotational equilibrium with the equilibrium constant, K, set equal to [o-isomer]/[i-isomer].

Table 1. Selected Thermodynamic Parameters for the Rotational Equilibrium of $[Cu(Mepypm)(diphosphine)]^+$ Complexes under Various Conditions

	solvent	ΔH^a	ΔS^b	$\Delta G_{298}{}^c$	$x_{o,298}{}^d$
$1{\cdot}BF_4$	$CDCl_3$	0.0	8	−2.6	74
$1{\cdot}BF_4$	CD_2Cl_2	1.3	11	−2.1	70
$1{\cdot}BF_4$	acetone-d_6	0.0	7	−2.1	70
$1{\cdot}BF_4$	CD_3CN	0.2	6	−1.6	65
$1{\cdot}B(C_6F_5)_4$	$CDCl_3$	−0.2	6	−2.2	71
$2{\cdot}BF_4$	$CDCl_3$	5.6	25	−1.9	68
$2{\cdot}BF_4$	CD_2Cl_2	4.0	15	−0.6	56
$2{\cdot}BF_4$	acetone-d_6	2.5	11	−0.8	58
$2{\cdot}BF_4$	CD_3CN	3.0	10	0.0	50
$2{\cdot}B(C_6F_5)_4$	$CDCl_3$	3.3	13	−0.7	57

[a]Enthalpy for i → o rotation,/kJ mol^{-1}. [b]Entropy for i → o rotation,/J K^{-1} mol^{-1}. [c]Gibbs free energy for i → o rotation at 298 K/kJ mol^{-1}. [d]Molar ratio of the o-isomer at 298 K/%.

The results reveal two key points: (a) the values of both ΔH and ΔS of $2{\cdot}BF_4$ in $CDCl_3$ were large and positive and (b) the values of $x_{o,298}$ were reduced in more polar solvents or with use of a larger counterion.

Both the enthalpy and entropy values for the rotation of $2{\cdot}BF_4$ in $CDCl_3$ (ΔH = 6 kJ mol^{-1} and ΔS = 25 J K^{-1} mol^{-1}) were more positive than that tested under other conditions (Table 1), such as in more polar solvents CD_2Cl_2 (ΔH = 4 kJ mol^{-1} and ΔS = 15 J K^{-1} mol^{-1}), acetone-d_6 (ΔH = 3 kJ mol^{-1} and ΔS = 10 J K^{-1} mol^{-1}), and CD_3CN (ΔH = 3 kJ mol^{-1} and ΔS = 10 J K^{-1} mol^{-1}). The parameters of $2{\cdot}B(C_6F_5)_4$ in $CDCl_3$

dx.doi.org/10.1021/ic302141z | Inorg. Chem. 2013, 52, 369−380

(ΔH = 3 kJ mol^{-1} and ΔS = 13 J K^{-1} mol^{-1}) were more negative than those of **2**·BF_4. On the other hand, the values of ΔH and ΔS of $\mathbf{1}^+$ under the same aforementioned conditions fell within ranges of 0−1 kJ mol^{-1} and 6−11 J K^{-1} mol^{-1}, respectively, indicating that the solvent and counterion effects on the values of both ΔH and ΔS of $\mathbf{1}^+$ were less than those of $\mathbf{2}^+$. In all tests, the values of ΔH and ΔS of $\mathbf{2}^+$, particularly ΔH, were more positive than those of $\mathbf{1}^+$. These results suggest that the diphosphine moieties considerably affect the enthalpy and entropy for the rotational isomerization.

A lower population of the o-isomer, particularly in $\mathbf{2}^+$, was observed when a larger counterion was employed. The $x_{o,298}$ values of **2**·BF_4 and **2**·$B(C_6F_5)_4$ in $CDCl_3$ were 68% and 57%, respectively. Significant counterion effects were not observed in $\mathbf{1}^+$; the ratio of **1**·$B(C_6F_5)_4$ in $CDCl_3$ ($x_{o,298}$ = 71%) is slightly less than that of **1**·BF_4 in $CDCl_3$ ($x_{o,298}$ = 74%). A lower population of the o-isomer in the polar solvent, similar to that observed in a previous report,[57] was found not only for **1**·BF_4 but also for **2**·BF_4. The values of $x_{o,298}$ for **2**·BF_4 in CD_2Cl_2, acetone-d_6, and CD_3CN were 56%, 58%, and 50%, respectively, which are less than the values obtained in $CDCl_3$. These trends are approximately observed in the full temperature range (see the van't Hoff plots in Figure 5). The population of the entropically favored o-isomer is reduced at lower temperature (x_o at 233 K = 54%; ΔG = −0.3 kJ mol^{-1}). The two isomers therefore have comparable stabilities. Because the values of ΔH under the other conditions were relatively small, the temperature dependences of x_o and ΔG were less significant than that for **2**·BF_4 in $CDCl_3$.

The parameters ΔH, ΔS, ΔG_{298}, and $x_{o,298}$ were plotted against the Kirkwood function,[17] $(\varepsilon_r - 1)/(2\varepsilon_r + 1)$, where ε_r corresponds to the relative permittivity of the solvent (Figure 6; ε_r = 4.89 for $CDCl_3$, 8.93 for CD_2Cl_2, 20.56 for acetone-d_6, and 35.94 for CD_3CN). Roughly linear relationships between the parameters and $(\varepsilon_r - 1)/(2\varepsilon_r + 1)$ indicate that the solvent polarity contributes considerably to the thermodynamics of the systems considered. The slopes of the four **2**·BF_4 plots, based on a linear least-squares regression fitting, were much larger than those of **1**·BF_4, suggesting that $\mathbf{2}^+$ is more sensitive to solvent selection than $\mathbf{1}^+$. The slopes of ΔG_{298} for both **1**·BF_4 and **2**·BF_4 are positive, indicating that the mechanism of the solvent dependency is similar throughout the [Cu(Mepypm)(diphosphine)]$^+$ family.

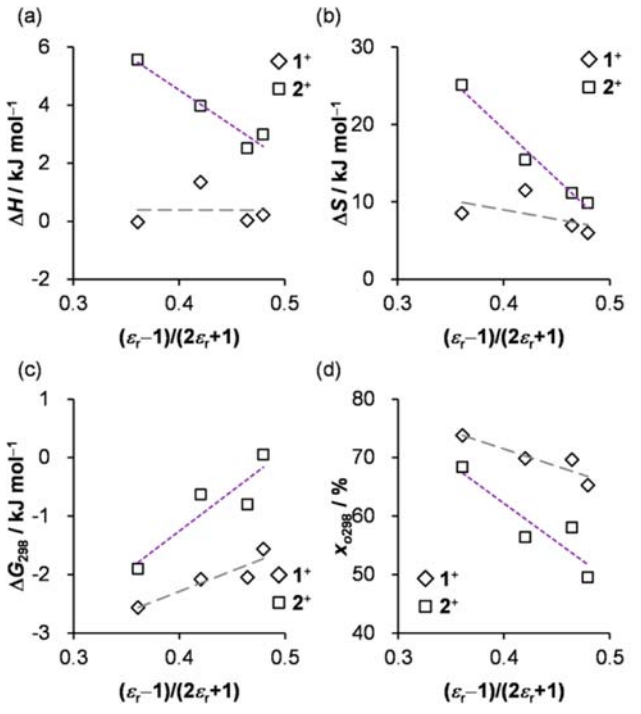

Figure 6. Correlation between the Kirkwood function, $(\varepsilon_r - 1)/(2\varepsilon_r + 1)$, and the thermodynamic parameters ΔH (a), ΔS (b), ΔG_{298} (c), and x_{o298} (d) of **1**·BF_4 and **2**·BF_4 in $CDCl_3$, CD_2Cl_2, acetone-d_6, and CD_3CN.

The aforementioned weak interaction dependence of the parameters ΔH, ΔS, ΔG_{298}, and $x_{o,298}$ cannot be explained by the simple consideration of chemical structures alone. For completeness, with the aid-generated crystal structures, we constructed a model that considers the geometries of both the ion pair and the six-membered chelating dppp moiety, as highlighted in the following section.

Discussion for the Thermodynamics of Rotation. The geometric features of $\mathbf{2}^+$ and reference compound $\mathbf{1}^+$ are illustrated at the top of Figure 7. The major bonding surface of the copper center in both $\mathbf{1}^+$ and $\mathbf{2}^+$ is occupied by the coordinating nitrogen atoms and diphosphine moiety. The bonding area taken up by coordination in $\mathbf{2}^+$ is reduced compared with that in $\mathbf{1}^+$, which provides additional space that a counterion or a methyl group on the pyrimidine moiety can occupy. Contributions of the CIP state in $CDCl_3$ are larger than those in more polar solvents such as CD_3CN.[17] In other words, the population of the SSIP state in a polar solvent is larger than that in a less polar solvent. For clarity, we focus on the representative two ion-pairing states and omit the others. It should be noted that ion pairing between a monovalent metal complex cation and a monovalent counteranion is strengthened in $CDCl_3$, moderate in CD_2Cl_2, and weakened in more polar solvents such as acetone-d_6.[23−26] On the other hand, with respect to the size of the anion, BF_4^- is significantly smaller than $B(C_6F_5)_4^-$, which is comparable with the size of the copper complex cation.

The value of ΔH for solvated i- and o-isomers is linked to intrinsic preference caused by the induction effect of the methyl group, electrostatic interactions, solvation, electrostatic attraction between the electron cloud of the methyl group and the positively charged metal core of the complex, and other enthalpic factors present. The ΔS values are a reflection of their respective freedom of rotation of the functional groups, along with the vibrational freedom of the ligand moieties, solvent, and counterion. For example, the large positive values of **2**·BF_4 in $CDCl_3$ indicate that the behavior of the solvated i-isomer differs significantly from the solvated o-isomer. In addition, the relatively small absolute values of both ΔH and ΔS of other conditions, **2**·BF_4 in a polar solvent, **1**·BF_4 in all solvents as we tested, **2**·$B(C_6F_5)_4$ in $CDCl_3$, and **1**·$B(C_6F_5)_4$ in $CDCl_3$, indicate that the differences in the behaviors between the solvated i- and o-isomers are trivial.

The rotational equilibrium in solution is represented as a model, displayed in Figure 7. Six conditions are represented: (a) **2**·BF_4 in $CDCl_3$, (b) **2**·BF_4 in CD_3CN, (c) **2**·$B(C_6F_5)_4$ in $CDCl_3$, (d) **1**·BF_4 in $CDCl_3$, (e) **1**·BF_4 CD_3CN, and (f) **1**·$B(C_6F_5)_4$ in $CDCl_3$. The equilibrium behaviors in CD_2Cl_2 and acetone-d_6 can be interpreted as a range from those in less polar $CDCl_3$ to those in more polar CD_3CN, considering their moderate values of ΔH, ΔS, ΔG, and relative permittivity. Each result has two points: (i) ΔH and ΔS; (ii) ΔG_{298} and $x_{o,298}$.

dx.doi.org/10.1021/ic302141z | Inorg. Chem. 2013, 52, 369−380

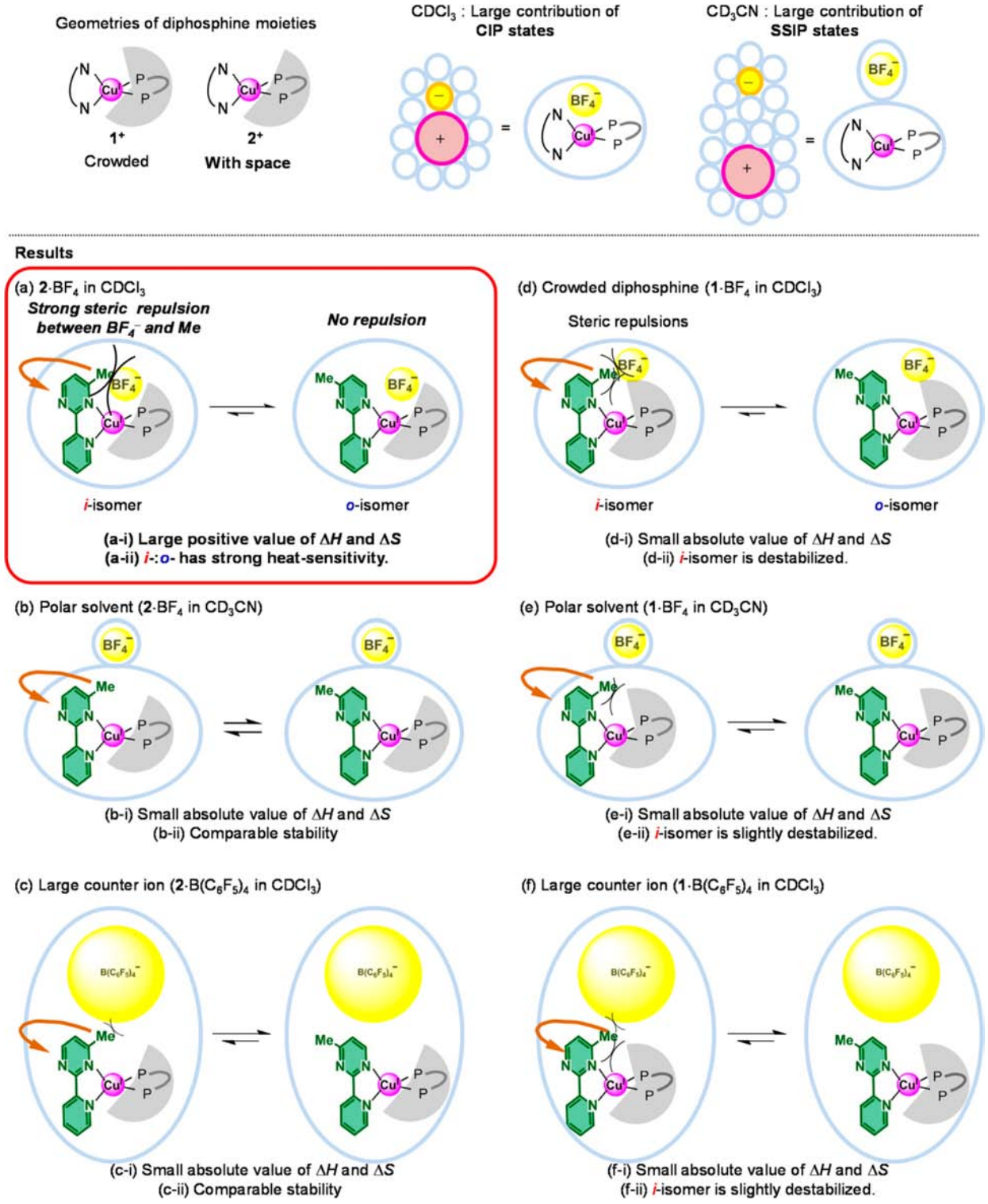

Figure 7. Illustrations of the effect of ion pairing on the rotational bistability of a $[Cu(Mepypm)(diphosphine)]^+$ family. (top, left) Geometric features of the diphosphine moieties of $\mathbf{1}^+$ and $\mathbf{2}^+$. (top, right) The copper(I) complexes in CIP and SSIP states. (a–f) Selected chemical equilibrium between the solvated i- and o-isomers: (a) $\mathbf{2}\cdot BF_4$ in $CDCl_3$; (b) $\mathbf{2}\cdot BF_4$ in CD_3CN; (c) $\mathbf{2}\cdot B(C_6F_5)_4$ in $CDCl_3$; (d) $\mathbf{1}\cdot BF_4$ in $CDCl_3$; (e) $\mathbf{1}\cdot BF_4$ in CD_3CN; (f) $\mathbf{1}\cdot B(C_6F_5)_4$ in $CDCl_3$.

Six Conditions a–f Explained as Follows. (a-i) The values of ΔH and ΔS of $\mathbf{2}\cdot BF_4$ in $CDCl_3$ are larger in magnitude and more positive than those under other conditions. In the CIP state of the o-isomer, there is no steric repulsion between the counterion and methyl group (Figure 7a). In contrast, the CIP state of the solvated i-isomer competes for the BF_4^- ion and methyl group on the pyrimidine moiety as a result of steric repulsion. This repulsion can be correlated to destabilization of the solvated i-isomer owing to the loss of freedom of motion in both the complex cation and counterion. The steric repulsion can cause more positive ΔH. The enhanced solvated i-isomer preference based on a combination

dx.doi.org/10.1021/ic302141z | Inorg. Chem. 2013, 52, 369–380

of several enthalpic factors described above can contribute to ΔH because its movement is strongly limited by the competition. (**a-ii**) The negative value of ΔG_{298} indicates that the population of the entropically favorable solvated o-isomer, mentioned in part a-i, is larger than that of the i-isomer at 298 K. At a low temperature such as 233 K, where the entropic factor is less dominant, both isomers have comparable stability. The comparable stabilization effects in the viewpoint of enthalpy and entropy cause the bistability based on the rotational equilibrium.

(**b-i**) The effects of solvent polarity are described in this paragraph. The ΔH and ΔS of **2**·BF_4 are positively small in polar solvents such as CD_3CN (Figure 7b). The steric repulsion between the counterion and methyl group on the pyrimidine moiety, mentioned in part a-i, is relatively small in the SSIP states of both the solvated i- and o-isomers. Therefore, the absolute values of ΔH and ΔS are also small.

(**b-ii**) The $x_{o,298}$ values of **2**·BF_4 in CD_3CN are smaller than those in $CDCl_3$ because destabilization of the solvated i-isomer, mentioned in paragraph a, is considerably minimized in the SSIP state.

(**c-i**) The effects of the counterion size are described in this paragraph. The ΔH and ΔS of **2**·$B(C_6F_5)_4$ in $CDCl_3$ are more negative than those of **2**·BF_4 in $CDCl_3$, which is characteristic of the other conditions (Figure 7c). Therefore, the $B(C_6F_5)_4^-$ ion causes a small destabilization of the i-isomer in the CIP state, as described in paragraph a, because of its size.

(**c-ii**) The inhibition of destabilization of the i-isomer also causes a decrease in $x_{o,298}$ for the $B(C_6F_5)_4^-$ ion compared with the BF_4^- ion.

(**d-i**) The effect of the geometry of the diphosphine ligand is described in paragraphs d–f. Despite the absolute values of ΔH and ΔS of **2**·BF_4 in $CDCl_3$ being relatively large, those of **1**·BF_4 in $CDCl_3$ are small because the bulkiness of the diphosphine of $\mathbf{1}^+$ reduces the steric repulsion between the counterion and methyl group of the solvated i-isomer, as mentioned in part a-i (Figure 7d). The reason for nearly zero ΔH value of $\mathbf{1}^+$ can be interpreted as a small difference in solvation between the i- and o-isomers (Figure 7d).

(**d-ii**) The value of ΔG_{298} is negative because the bulkiness of the diphosphine contributes to destabilization of the i-isomer via steric repulsion between the methyl group and diphosphine moiety. The bulkiness is also the reason why $x_{o,298}$ of **1**·BF_4 in several solvents is larger than that of **2**·BF_4.

(**e-i**) The absolute values of both ΔH and ΔS of **1**·BF_4 in CD_3CN are small because of a combination of phenomena described in parts b-i and d-i (Figure 7e).

(**e-ii**) The negative ΔG stems from the steric bulk of the diphosphine as described in part d-ii. The lower $x_{o,298}$ of **1**·BF_4 in polar solvents compared with that of **1**·BF_4 in $CDCl_3$ was attributed to ion-pairing effects, as highlighted in the above comparison of parts a and b.

(**f-i**) The absolute values of both ΔH and ΔS of **1**·$B(C_6F_5)_4$ in $CDCl_3$ are small due to a combination of the c-i and d-i phenomena (Figure 7f).

(**f-ii**) Because the ion-pairing effects are slightly retained, $x_{o,298}$ of **1**·$B(C_6F_5)_4$ was lower than that of **1**·BF_4.

The values of both ΔH and ΔS contain a contribution of the effects mentioned above as well as the following intrinsic factors. For example, stabilization of the i-isomer stemming from the electronic structure of Mepypm, which can be derived from induction effects, thus contribute to positive ΔH values. Stabilization of the i-isomer caused by an easing of the C–H interaction between the methyl group and the phenyl groups on the diphosphine can also contribute to positive ΔH values. The entropy loss of the i-isomer originates from a crowded coordination geometry, which reduces the freedom of motion of the ligand moiety, thus contributing to positive values of ΔS. The intrinsic factors also contribute to the values of x_o.

Consequently, all results related to thermodynamics can be reasonably understood based on the proposed model, suggesting that the present rotational bistability, particularly in $\mathbf{2}^+$, arises from solvated ion pairing.

Notes about the Model. It should be noted that the ^1H NMR signals can be the average of many kinds of conformations with negligible differences in chemical shifts, such as the resonances of the solvent, counterion, and ligands including the diphosphine moiety. The conceptual diagrams, displayed in Figure 7, are representative of the real equilibrium. Because the crystal structures of the $[Cu(Mepypm)(diimine)]^+$ family[53] were very different from those of the present complexes, particularly from the viewpoint of the coordination structure and location of the counterion, the ion-pairing sensitivity is characteristic of $[Cu(Mepypm)(diphosphine)]^+$ structures.

Changes in the dipole moment, hydrogen-bonding interaction, and hydrophobic interactions between states are often attributed to solvent sensitivity not only in traditional axial/equatorial conformational equilibrium[17] but also in chemistry for promising nanomaterials such as molecular machines based on supramolecules.[7,8,71–74] Because the i- and o-isomers are similar with respect to the coordination structure, the polarity differences between the complex cations of the two isomers are expected to be small. On the other hand, the absolute value of the dipole moment of the solvated copper(I) compounds is expected to be proportional to the distance between the copper atom and counterion center (Cu–X). Therefore, the polarity of the i-isomer in the CIP state is expected to be larger than that of the o-isomer, considering that the Cu–X distance is determined by steric repulsion. This is an additional effect caused by ion pairing, as described in Figure 7. The difference in polarity between the two isomers in the CIP state can contribute to the preference of the i-isomer for a more polar solvent. This rationale is incomplete for three reasons: (1) the population of the CIP state in the polar solvent is small, (2) the difference of the Cu–X distance between i- and o-isomers in the SSIP state is small, and (3) the large ΔH and ΔS of **2**·BF_4 in $CDCl_3$ cannot be appropriately explained by this reasoning.

If a solvent molecule, such as CD_3CN, coordinates to the copper(I) center, steric repulsion between the methyl group and solvent molecule would cause a decrease of the i-isomer ratio in CD_3CN compared with $CDCl_3$. This assumption can be totally denied because of both the experimental results and copper(I) electronic configuration. The copper(I) center already has a coordination number of 4, so it cannot accommodate any additional ligand.

We assume that the volume occupied by $\mathbf{2}^+$ (Figure 7) can be modified in $CDCl_3$, which can destabilize the i-isomer via steric repulsion between the methyl group and solvent molecule. Because this assumption does not explain the decrease in the o-isomer molar ratio when a larger counterion is used, the effects of the size of the solvent molecule are small.

Rate for Isomerization in a Solution State. The rate constants for the i → o isomerization, k, at variable temperature were estimated from Arrhenius plots based on simulation of the broadened ^1H NMR spectra (Figure 8 and the Supporting

dx.doi.org/10.1021/ic302141z | Inorg. Chem. 2013, 52, 369–380

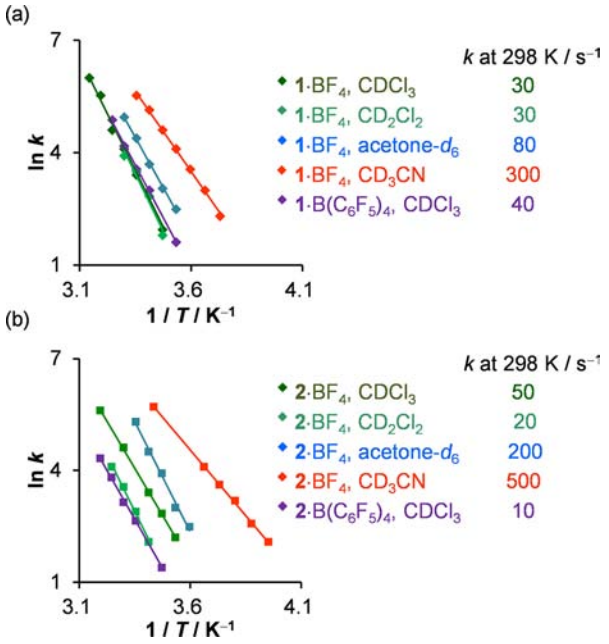

Figure 8. Arrhenius plots and rate constant at 298 K for the i → o interconversion of $\mathbf{1}^+$ (a) and $\mathbf{2}^+$ (b) under a variety of conditions.

Information, Figures S1–S10). The values of k at 298 K, k_{298}, which are the parameters most representative of the solvent- and counterion-sensitive kinetics, are also summarized in Figure 8. Other parameters are tabulated in the Supporting Information, Table S3.

Kinetic analysis supports the validity of thermodynamic analysis. The magnitude of the k values at the given temperature, where ^{1}H NMR spectra for thermodynamic analysis were conducted, falls within a range of 10^{-2}–10^{0} s^{-1} (Supporting Information, Figure S18). Qualitatively, the values indicate that the system reaches equilibrium within 10^2 s. For the ^{1}H NMR spectra conducted with ca. 10^3 s intervals, the signal integrations reflect the ratio of the i- and o-isomers in equilibrium. Signal broadening is observed when k exceeds ca. 10^1 s^{-1}. The ^{1}H NMR spectra at high temperature are not employed for thermodynamic analysis.

The much larger k_{298} values obtained in coordinating solvent such as CD_3CN, compared with noncoordinating solvents such as $CDCl_3$, were observed not only for $\mathbf{1}\cdot BF_4$[57] but also for $\mathbf{2}\cdot BF_4$ (50 s^{-1} in $CDCl_3$, 20 s^{-1} in CD_2Cl_2, 200 s^{-1} in acetone-d_6, and 500 s^{-1} in CD_3CN). The promotion of isomerization by a coordinating solvent molecule, which assists the dissociation of the pyrimidine nitrogen atoms from the copper center,[57] was generally found throughout the [Cu(Mepypm)(diphosphine)]$^+$ family. The rate constant associated with $\mathbf{1}\cdot BF_4$ in CD_2Cl_2 (k_{298} = 30 s^{-1}) was comparable with that of $\mathbf{1}\cdot BF_4$ in $CDCl_3$ because the coordination abilities of these solvents are similarly weak. In contrast, a small decrease of k_{298} in CD_2Cl_2 compared with $CDCl_3$ was observed for $\mathbf{2}\cdot BF_4$. The solvent sensitivity seems to be consistent with the model illustrating that the ion-pairing sensitivity of $\mathbf{2}^+$ is larger than that of $\mathbf{1}^+$, shown in Figure 7. The value of k_{298} in a $CDCl_3$ solution of $\mathbf{2}\cdot B(C_6F_5)_4$ is 10 s^{-1}, which is smaller than that of $\mathbf{2}\cdot BF_4$. The decrease of k_{298} resulting from the use of a bulky counteranion suggests that the weak coordination ability of BF_4^- can slightly assist in Cu–N bond dissociation. This behavior seems to be consistent with the model describing the BF_4^- ion approach in the CIP state. $\mathbf{1}\cdot B(C_6F_5)_4$ in $CDCl_3$ (k_{298} = 40 s^{-1}) is very similar to $\mathbf{1}\cdot BF_4$ in $CDCl_3$. The resemblance also seems to relate to the model provided in Figure 7. The CIP effect can contribute to the kinetics of rotation, but this effect seems to be smaller than that of the solvent coordination. The solvent sensitivity trends, mentioned above, are basically observed over the full temperature range tested (see the Arrhenius plots in Figure 8). The k value varied from 10^{-6} s^{-1} (frozen motion) to 10^3 s^{-1} over the temperature and solvent ranges considered (Supporting Information, Figure S18). These slow rates, compared to many of chemical equilibrium, are one of the requirements for switching between equilibrium and metastable states, which play a key role for our systems with electric signal response.

Physical Properties of $\mathbf{2}^+$. In our previous systems, [Cu(Mepypm)(L_{anth})]$^+$ and their derivatives were found to exhibit reversible copper(II/I) redox activities that were synchronized with rotational isomerization.[53−55,58] Cyclic voltammograms of $\mathbf{2}\cdot BF_4$ in 0.1 M Bu_4NBF_4–CH_2Cl_2 show irreversible oxidation waves at approximately 0.7 V vs Ag^+/Ag (Figure 9a). This irreversibility seems to be caused by an instability of the oxidized [Cu(Mepypm)(diphosphine)]$^+$, which can undergo rapid adverse chemical reactions. Redox irreversibility is also observed in some [Cu(diimine)(diphosphine)]$^+$ complexes.[42] The redox potential in a solution with $B(C_6F_5)_4^-$ is more positive than that with BF_4^-, and the reversibility of the redox wave in the solution with $B(C_6F_5)_4^-$ is better than that with BF_4^- (Figure 9a). Stabilization of the oxidized form by noncoordinative bulky $B(C_6F_5)_4^-$ could attribute to these results. The electrolyte effects of $B(C_6F_5)_4^-$ on the reversibility of some simple redox-active molecules have been reported in the literature.[79]

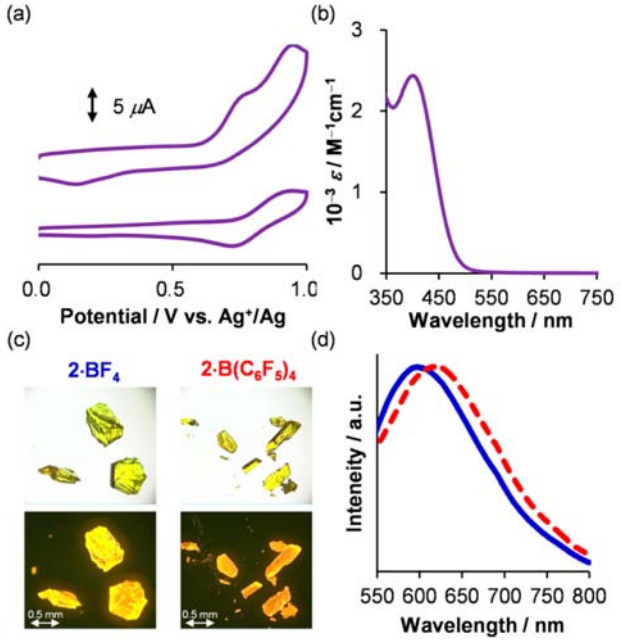

Figure 9. (a) Cyclic voltammogram of $\mathbf{2}\cdot BF_4$ (0.4 mM) in 0.1 M Bu_4NBF_4–CH_2Cl_2 (top) and $\mathbf{2}\cdot B(C_6F_5)_4$ (0.4 mM) in 0.1 M $Bu_4NB(C_6F_5)_4$–CH_2Cl_2 (bottom) at room temperature at a scan rate of 100 mV s^{-1}. (b) Absorption spectrum of $\mathbf{2}\cdot BF_4$ in acetone at room temperature. (c) Fluorescence microscopy images of solids of $\mathbf{2}\cdot BF_4$ (left) and $\mathbf{2}\cdot B(C_6F_5)_4$ (right) in a bright field (top) and under blue-light excitation (bottom) at room temperature. (d) Emission spectra of $\mathbf{2}\cdot BF_4$ (blue) and $\mathbf{2}\cdot B(C_6F_5)_4$ (red, dotted line) in the solid state at room temperature.

dx.doi.org/10.1021/ic302141z | Inorg. Chem. 2013, 52, 369–380

The environment-sensitive molar ratio of rotational isomers can cause negligible change in absorption in solution. The UV−vis absorption spectrum of **2**·BF_4 in acetone displayed a charge-transfer (CT) absorption band characteristic of [Cu(diimine)(diphosphine)]$^+$ complexes (Figure 9b). The maximum wavelength (λ_{max}) and the molar extinction coefficient (ε) at λ_{max} of the CT absorption were 401 nm and 2.4 × 10^3 M^{-1} cm^{-1}, respectively. The red shift of the absorption maximum of **2**·BF_4 compared with **1**·BF_4[57] is caused by previously reported diphosphine effects.[44,47,49] The absorption maximum wavelengths of **2**·BF_4 and **2**·$B(C_6F_5)_4$ in acetone were identical (Supporting Information, Figure S19). Because the effects of methyl substitution on the absorption maxima of copper(I) diimine complexes are known to be within a few nanometers,[44,50] the difference in absorption between the i- and o-isomers is also expected to be small. The small difference in color is consistent with our previous findings pertaining to the methylpyrimidine-based rotational isomers.[53,58] The luminescence of **2**·BF_4 and **2**·$B(C_6F_5)_4$ in acetone at room temperature, which is the same experimental condition as that reported for the luminescence of **1**$^+$,[58] was not detected; luminescence quantum yields of **1**·BF_4 and **2**·BF_4 were 0.02% and less than 0.002%, respectively. The negligible luminescence of **2**$^+$ compared with **1**$^+$ is attributed to the different steric demands of the two diphosphines; DPEphos offers an enhanced protection toward structural deformations in both the ground and excited states and additionally blue-shifts the absorption through electronic effects, leading to a better emission performance for **1**$^+$.[43−47] The values of the luminescence quantum yields are consistent with the well-established photophysics of a family of [Cu(diimine)(diphosphine)][43−47] because of the large structural rearrangement that occurs in the photoexcited state of complexes containing less bulky Mepypm ligands compared with bulky diimines such as 2,9-dimethyl-1,10-phenanthroline[44,47] and the high possibility of solvent coordination quenching due to the presence of the less bulky Mepypm.[44,47] Solids of **2**·BF_4 and **2**·$B(C_6F_5)_4$ were yellow on appearance and exhibited orange luminescence under UV and blue-light excitation (Figure 9c). The emission spectra of **2**·BF_4 and **2**·$B(C_6F_5)_4$ solids displayed CT luminescence characteristic of [Cu(diimine)(diphosphine)]$^+$ systems (Figure 9d).[36−41,47] The maximum emission wavelength of **2**·BF_4 (λ_{max} = 597 nm) was blue-shifted compared with that of **2**·$B(C_6F_5)_4$ (λ_{max} = 620 nm; Figure 9d). An enhancement in the solid-state luminescence over the solution luminescence, which is typical for emissive copper(I) diimine complexes, was observed. The enhancement is attributed to inhibited structural relaxation in the solid state and/or additional solvent coordination to photoexcited species that occur in solution.[39−41] The differences in the orientation of the pyrimidine ring, position of the counterion, and other types of packing effects can contribute to the blue shift of **2**·BF_4 relative to **2**·$B(C_6F_5)_4$.[39,40,51,52]

CONCLUSION

A series of simple copper(I) complexes bearing Mepypm and diphosphine ligands, namely, **1**·$B(C_6F_5)_4$, **2**·BF_4, and **2**·$B(C_6F_5)_4$, were synthesized. Two rotational isomers of the complexes coexist and interconvert in solution via intramolecular ligating atom exchange of the pyrimidine ring, as previously reported for **1**·BF_4. The values of ΔH, ΔS, and ΔG for rotation are strongly dependent on the steric demands of the diphosphine, polarity of the solvent, and size of the counterion. Consideration of solvated counterion pairing is key for rationally accounting for the effect of the weak interaction on the rotational equilibrium. Because the major part of the copper center bonding surface was occupied by ligands, the position of the counterion affects the orientation of the pyrimidine moiety. The findings described herein are valuable for the design of photoactive and/or redox-active molecular mechanical units that can be readily functionalized via weak electrostatic interactions.

EXPERIMENTAL SECTION

Materials. **1**·BF_4 was obtained by methods described previously.[57] 4-Methyl-2-(2′-pyridyl)pyrimidine (Mepypm),[80] tetrakis(acetonitrile)copper(I) tetrafluoroborate ([Cu(MeCN)$_4$]BF_4),[64] and tetrakis(acetonitrile)copper(I) tetrakis(pentafluorophenyl)borate ([Cu(MeCN)$_4$]$B(C_6F_5)_4$)[65] were prepared according to literature protocols. Bis[2-(diphenylphosphino)phenyl] ether (DPEphos) was purchased from Wako Pure Chemical Industries, Ltd. 1,3-Bis(diphenylphosphino)propane (dppp) was purchased from Kanto Chemicals. Other chemicals were used as purchased.

Synthesis of [Cu(Mepypm)(DPEphos)]$B(C_6F_5)_4$ [1·$B(C_6F_5)_4$]. The heteroleptic copper complex **1**·$B(C_6F_5)_4$ was synthesized according to a modified literature procedure.[44,47,57] In this synthesis, [Cu(MeCN)$_4$]$B(C_6F_5)_4$ (80 mg, 0.088 mmol) was added to DPEphos (59 mg, 0.11 mmol) in 5 mL of dichloromethane. Mepypm (14 mg, 0.082 mmol) in 5 mL of dichloromethane was then added, upon which the reaction solution immediately turned yellow. The reaction mixture was subsequently stirred for an additional 30 min. Hexane was then added to the solution in order to precipitate the product as a yellow solid, which was filtered and washed with hexane. Reprecipitation from a dichloromethane and hexane mixture afforded **1**·$B(C_6F_5)_4$ as a yellow solid with a yield of 70% (83 mg). ^{1}H NMR (500 MHz, $CDCl_3$, 253 K): δ 8.76 (m, o-1H + i-1H), 8.68 (d, J = 7.7 Hz, i-1H), 8.37 (d, J = 5.5 Hz, o-1H), 8.29 (d, J = 5.5 Hz, o-1H), 8.26 (d, J = 4.8 Hz, i-1H), 7.99 (t, J = 7.8 Hz, o-1H), 7.95 (t, J = 7.6 Hz, i-1H), 7.4−6.7 (m), 2.63 (s, o-3H), 2.29 (s, i-3H). Elem anal. Calcd for $C_{70}H_{37}N_3P_2OCuBF_{20}$: C, 57.89; H, 2.57; N, 2.89. Found: C, 58.16; H, 2.87; N, 2.77.

Synthesis of [Cu(Mepypm)(dppp)]BF_4 (2·BF_4). **2**·BF_4 was synthesized using a procedure similar to that described for **1**·$B(C_6F_5)_4$ with the exception that diethyl ether was used in place of hexane. [Cu(MeCN)$_4$]BF_4 (67 mg, 0.21 mmol), dppp (104 mg, 0.25 mmol), and Mepypm (34 mg, 0.20 mmol) were used. Yield: yellow solid (56%, 82 mg). ^{1}H NMR (500 MHz, $CDCl_3$, 253 K): δ 8.97 (d, J = 5.0 Hz i-1H), 8.93 (d, J = 7.9 Hz, i-1H), 8.85 (d, J = 7.9 Hz, o-1H), 8.79 (d, J = 5.5 Hz, o-1H), 8.47 (d, J = 5.1 Hz, o-1H), 8.35 (d, J = 5.2 Hz, i-1H), 8.20 (t, J = 7.8 Hz, i-1H), 8.11 (t, J = 7.7 Hz, o-1H), 7.69 (dd, J = 7.5 and 5.1 Hz, i-1H), 7.62 (dd, J = 7.5 and 5.2 Hz, o-1H), 7.5−7.1 (m), 2.88 (m, br), 2.7 (br), 2.69 (s, o-3H), 2.45 (t, br), 2.32 (s, i-3H), 2.10 (m, br). Elem anal. Calcd for $C_{37}H_{35}N_3P_2CuBF_4$: C, 60.54; H, 4.81; N, 5.73. Found: C, 60.52; H, 4.92; N, 5.49.

Synthesis of [Cu(Mepypm)(dppp)]$B(C_6F_5)_4$ [2·$B(C_6F_5)_4$]. **2**·$B(C_6F_5)_4$ was synthesized using a procedure similar to that described for **1**·$B(C_6F_5)_4$ by employing [Cu(MeCN)$_4$]$B(C_6F_5)_4$ (185 mg, 0.20 mmol), dppp (92 mg, 0.22 mmol), and Mepypm (35 mg, 0.20 mmol). Yield: yellow solid (40%, 108 mg). ^{1}H NMR (500 MHz, $CDCl_3$, 253 K): δ 8.91 (d, J = 8.0 Hz, i-1H), 8.88 (m, i-1H + o-1H), 8.29 (d, J = 5.1 Hz, o-1H), 8.26 (d, J = 4.7 Hz, i-1H), 8.18 (d, J = 5.5 Hz, o-1H), 8.14 (t, J = 7.8 Hz, i-1H), 8.09 (t, J = 7.9 Hz, o-1H), 7.59 (dd, J = 7.4 and 5.3 Hz, i-1H), 7.50 (dd, J = 7.3 and 5.4 Hz, o-1H), 7.4−7.1 (m), 2.87 (m, br), 2.7 (br), 2.69 (s, o-3H), 2.57 (m, br), 2.35 (m, br), 2.23 (s, i-3H), 2.14 (m, br). Elem anal. Calcd for $C_{61}H_{35}N_3P_2CuBF_{20}$: C, 55.24; H, 2.66; N, 3.17. Found: C, 55.10; H, 2.86; N, 3.13.

X-ray Structural Analysis. Yellow single crystals of o-**1**·$B(C_6F_5)_4$·1.5hexane, o-**2**·BF_4·0.5MeOH, and i-**2**·$B(C_6F_5)_4$ were obtained by the slow diffusion of hexane into a dichloromethane solution of **1**·$B(C_6F_5)_4$, diethyl ether into a methanol solution of **2**·BF_4, and hexane into a chloroform solution of **2**·$B(C_6F_5)_4$, respectively. Diffraction data were collected on an AFC10 diffractometer with graphite-monochromated Mo Kα radiation (λ = 0.7107 Å). Lorentz polarization and numerical absorption corrections were performed

dx.doi.org/10.1021/ic302141z | Inorg. Chem. 2013, 52, 369−380

with the *CrystalClear 1.3.6* program. The structure was solved by direct methods using *SIR 92* software[81] and refined against F^2 using *SHELXL-97*.[82] *WinGX* software was used to prepare the material for publication.[83] Crystallographic data are listed in the Supporting Information, Table S1. Disordered counterions in o-**2**·BF_4·0.5MeOH were analyzed by the *PART*, *SIMU*, and *SADI* options of *SHELXL-97*.[82] The disordered methanol molecule in o-**2**·BF_4·0.5MeOH was analyzed by the *PART*, *EADP*, and *SADI* options of *SHELXL-97*.[82]

Instruments. NMR spectra at several temperatures in the dark were recorded on a Bruker DRX 500 spectrometer, using a ca. 20 min data-recording interval. The experimental ^{1}H NMR spectra were simulated using *iNMR 2.6.5* software. The reported chemical shifts of the solvent peaks were used for calibration of the NMR spectra in $CDCl_3$ (tetramethylsilane, δ 0), CD_2Cl_2 (δ 5.32), acetone-d_6 (δ 2.05), and acetonitritrile-d_3 (CD_3CN, δ 1.94).[84] UV−vis absorption spectra were recorded with a Hewlett-Packard 8453 spectrometer. Steady-state-corrected emission spectra were obtained with a Hitachi F-4500 spectrometer. The luminescence quantum yield was estimated from tris(2,2′-bipyridine)ruthenium(II) hexafluorophosphate in acetonitrile under air (1.8%) as a standard.[85] Solid-state luminescence images were measured under blue-light excitation using an Olympus BX51 fluorescence microscope. Electrochemical measurements were acquired with an ALS 750A electrochemical analyzer (BAS Co. Ltd.). The working electrode was a 0.3-mm-o.d. glassy carbon electrode; a platinum wire served as the auxiliary electrode, and the reference electrode was an Ag^+/Ag electrode (a silver wire immersed in 0.1 M Bu_4NClO_4/0.01 M $AgClO_4$/CH_3CN). The solutions were deoxygenated with argon prior to measurement.

Thermodynamic and Kinetic Analyses. Analysis was performed using the aromatic ^{1}H NMR signals of the Mepypm moiety. The results of **1**·BF_4 in $CDCl_3$, acetone-d_6, and CD_3CN were comparable with previously reported values, which were based on the methyl group of the Mepypm moiety.[57] The solution-state molar ratios of the isomers at several temperatures were determined from ^{1}H NMR signal integration. The broad spectra acquired at room temperature were excluded from thermodynamic analysis. The generated van't Hoff plots[86] were based on an equilibrium constant corresponding to the value of [o-isomer]/[i-isomer]. The molar ratios of the o-isomers, x_o, at variable temperatures were calculated by extrapolation of the van't Hoff plots. The thermodynamic parameters for the i → o rotation (ΔH, ΔS, and ΔG), K, and x_o can be represented by the following van't Hoff equations:

$$\ln[x_o/(100 - x_o)] = \ln K = -\Delta G/RT = -\Delta H/RT + \Delta S/R \quad (1)$$

Here, T corresponds to the absolute temperature and R is the gas constant (8.314 J K^{-1} mol^{-1}). The value of $x_{o,298}$ was estimated from the predicted value of ln K at $1/T$ = 1/298 K^{-1} using single linear regression of the van't Hoff plots. The error of $x_{o,298}$ was less than 1%, based on the root-mean-square error and t test in 95% significance level. The rate constants for the i → o isomerization, k, at several temperatures were determined from simulation analysis of the NMR spectra using the equilibrium constants determined from the van't Hoff plots. k values at variable temperatures were calculated by extrapolation of the Arrhenius plots:[86]

$$\ln k = -E_a/RT + \ln(A) \quad (2)$$

Here, E_a and A correspond to the activation energy and frequency factor of the i → o isomerization, respectively.

■ ASSOCIATED CONTENT

Supporting Information

Crystal structure data in CIF format (CCDC 902739, 902740, and 902741) and spectral data. This material is available free of charge via the Internet at http://pubs.acs.org. Crystallographic data can be obtained free of charge from The Cambridge Crystallographic Data Centre via www.ccdc.cam.ac.uk/data_request/cif.

■ AUTHOR INFORMATION

Corresponding Author

*E-mail: kume@chem.s.u-tokyo.ac.jp (S.K.), nisihara@chem.s.u-tokyo.ac.jp (H.N.).

Present Address

†Department of Chemistry, Graduate School of Science, Hiroshima University, 1-3-1 Kagamiyama, Higashi-Hiroshima 739-8526, Japan.

Notes

The authors declare no competing financial interest.

■ ACKNOWLEDGMENTS

This work was supported by Grants-in-Aid from MEXT of Japan [Grants 20750044, 20245013, and 21108002; area 2107 (Coordination Programming)], JST (Research Seeds Quest Program), a Research Fellowship of the Japan Society for the Promotion of Science for Young Scientists, and the Global COE Program for Chemistry Innovation.

■ REFERENCES

(1) Marcus, R. A. *J. Phys. Chem. B* **1998**, *102*, 10071−10077.
(2) Kavarnos, G. J.; Turro, N. J. *Chem. Rev.* **1986**, *86*, 401−449.
(3) Wasielewski, M. R. *Chem. Rev.* **1992**, *92*, 435−461.
(4) (a) Rueping, M.; Uria, U.; Lin, M.-Y.; Atodiresei, I. *J. Am. Chem. Soc.* **2011**, *133*, 3732−3735. (b) Rauniyar, V.; Lackner, A. D.; Hamilton, G. L.; Toste, F. D. *Science* **2011**, *334*, 1681−1684.
(5) Macchioni, A. *Chem. Rev.* **2005**, *105*, 2039−2073.
(6) (a) Imahori, H.; Tamaki, K.; Guldi, D. M.; Luo, C.; Fujitsuka, M.; Ito, O.; Sakata, Y.; Fukuzumi, S. *J. Am. Chem. Soc.* **2001**, *123*, 2607−2617. (b) D'Souza, F.; Chitta, R.; Ohkubo, K.; Tasior, M.; Subbaiyan, N. K.; Zandler, M. E.; Rogacki, M. K.; Gryko, D. T.; Fukuzumi, S. *J. Am. Chem. Soc.* **2008**, *130*, 14263−14272.
(7) Balzani, V.; Credi, A.; Venturi, M. *Molecular Devices and Machines*, 2nd ed.; Wiley-VCH: Weinheim, Germany, 2008.
(8) Kay, E. R.; Leigh, D. A.; Zerbetto, F. *Angew. Chem., Int. Ed.* **2007**, *46*, 72−191.
(9) Laursen, B. W.; Nygaard, S.; Jeppesen, J. O.; Stoddart, J. F. *Org. Lett.* **2004**, *6*, 4167−4170.
(10) Credi, A.; Dumas, S.; Silvi, S.; Venturi, M.; Arduini, A.; Pochini, A.; Secchi, A. *J. Org. Chem.* **2004**, *69*, 5881−5887.
(11) Gibson, H. W.; Jones, J. W.; Zakharov, L. N.; Rheingold, A. L.; Slebodnick, C. *Chem.—Eur. J.* **2011**, *17*, 3192−3206.
(12) Evans, N. H.; Rahman, H.; Leontiev, A. V.; Greenham, N. D.; Orlowski, G. A.; Zeng, Q.; Jacobs, R. M. J.; Serpell, C. J.; Kilah, N. L.; Davis, J. J.; Beer, P. D. *Chem. Sci.* **2012**, *3*, 1080−1089.
(13) Kim, S. K.; Sessler, J. L.; Gross, D. E.; Lee, C.-H.; Kim, J. S.; Lynch, V. M.; Delmau, L. H.; Hay, B. P. *J. Am. Chem. Soc.* **2010**, *132*, 5827−5836.
(14) Jones, J. W.; Gibson, H. W. *J. Am. Chem. Soc.* **2003**, *125*, 7001−7004.
(15) Tobey, S. L.; Anslyn, E. V. *J. Am. Chem. Soc.* **2003**, *125*, 10963−10970.
(16) Hou, J.; Zhang, Z.; Madsen, L. A. *J. Phys. Chem. B* **2011**, *115*, 4576−4582.
(17) Reichardt, C. *Solvents and Solvent Effects in Organic Chemistry*, 3rd ed.; Wiley-VCH: Weinheim, Germany, 2003.
(18) Meyer, T. J. *Acc. Chem. Res.* **1989**, *22*, 163−170.
(19) Park, J.; Pasupathy, A. N.; Goldsmith, J. I.; Chang, C.; Yaish, Y.; Petta, J. R.; Rinkoski, M.; Sthena, J. P.; Abruña, H. D.; McEuen, P. L.; Ralph, D. C. *Nature* **2002**, *417*, 722−725.
(20) Collin, J.-P.; Dietrich-Buchecker, C.; Gaviña, P.; Jiménez-Molero, M. C.; Sauvage, J.-P. *Acc. Chem. Res.* **2001**, *34*, 477−487.
(21) Armaroli, N.; Balzani, V.; Collin, J.-P.; Gavina, P.; Sauvage, J.-P.; Ventura, B. *J. Am. Chem. Soc.* **1999**, *121*, 4397−4408.
(22) Poleschak, I.; Kern, J. M.; Sauvage, J.-P. *Chem. Commun.* **2004**, 474−476.

(23) Pregosin, P. S.; Kumar, P. G. A.; Fernández, I. *Chem. Rev.* **2005**, *105*, 2977−2998.
(24) Moreno, A.; Pregosin, P. S.; Veiros, L. F.; Albinati, A.; Rizzato, S. *Chem.—Eur. J.* **2009**, *15*, 6848−6862.
(25) Kumar, P. G. A.; Pregosin, P. S.; Goicoechea, J. M.; Whittlesey, M. K. *Organometallics* **2003**, *22*, 2956−2960.
(26) (a) Rezende, M. C.; Guerrero, J. *Magn. Reson. Chem.* **2009**, *47*, 505−510. (b) Martinez-Viviente, E.; Pregosin, P. S. *Inorg. Chem.* **2003**, *42*, 2209−2214.
(27) Lacour, J.; Moraleda, D. *Chem. Commun.* **2009**, 7073−7089.
(28) Hebbe-Viton, V.; Desvergnes, V.; Jodry, J. J.; Dietrich-Buchecker, C.; Sauvage, J.-P.; Lacour, J. *Dalton Trans.* **2006**, 2058−2065.
(29) Desvergnes-Breuil, V.; Hebbe, V.; Dietrich-Buchecker, C.; Sauvage, J.-P.; Lacour, J. *Inorg. Chem.* **2003**, *42*, 255−257.
(30) Hutin, M.; Nitschke, J. R. *Chem. Commun.* **2006**, 1724−1726.
(31) Riesgo, E.; Hu, Y.-Z.; Bouvier, F.; Thummel, R. P. *Inorg. Chem.* **2001**, *40*, 2541−2546.
(32) Frei, U. M.; Geier, G. *Inorg. Chem.* **1992**, *31*, 187−190.
(33) Kume, S.; Murata, M.; Ozeki, T.; Nishihara, H. *J. Am. Chem. Soc.* **2005**, *127*, 490−491.
(34) Umeki, S.; Kume, S.; Nishihara, H. *Chem. Lett.* **2010**, *39*, 204−205.
(35) Kume, S.; Kurihara, M.; Nishihara, H. *Inorg. Chem.* **2003**, *42*, 2194−2196.
(36) Armaroli, N.; Accorsi, G.; Cardinali, F.; Listorti, A. *Top. Curr. Chem.* **2007**, *280*, 69−115.
(37) Lavie-Cambot, A.; Cantuel, M.; Leydet, Y.; Jonusauskas, G.; Bassani, D. M.; McClenaghan, N. D. *Coord. Chem. Rev.* **2008**, *252*, 2572−2584.
(38) McMillin, D. R.; McNett, K. M. *Chem. Rev.* **1998**, *98*, 1201−1219.
(39) (a) Zhang, Q.; Zhou, Q.; Cheng, Y.; Wang, L.; Ma, D.; Jing, X.; Wang, F. *Adv. Mater.* **2004**, *16*, 432−436. (b) Armaroli, N.; Accorsi, G.; Holler, M.; Moudam, O.; Nierengarten, J.-F.; Zhou, Z.; Wegh, R. T.; Welter, R. *Adv. Mater.* **2006**, *18*, 1313−1316.
(40) Hsu, C.-W.; Lin, C.-C.; Chung, M.-W.; Chi, Y.; Lee, G.-H.; Chou, P.-T.; Chang, C.-H.; Chen, P.-Y. *J. Am. Chem. Soc.* **2011**, *133*, 12085−12099.
(41) Smith, C. S.; Branham, C. W.; Marquardt, B. J.; Mann, K. R. *J. Am. Chem. Soc.* **2010**, *132*, 14079−14085.
(42) Linfoot, C. L.; Richardson, P.; Hewat, T. E.; Moudam, O.; Forde, M. M.; Collins, A.; White, F.; Robertson, N. *Dalton Trans.* **2010**, *39*, 8945−8956.
(43) Cuttell, D. G.; Kuang, S. M.; Fanwick, P. E.; McMillin, D. R.; Walton, R. A. *J. Am. Chem. Soc.* **2002**, *124*, 6−7.
(44) Kuang, S. M.; Cuttell, D. G.; McMillin, D. R.; Fanwick, P. E.; Walton, R. A. *Inorg. Chem.* **2002**, *41*, 3313−3322.
(45) Yang, L.; Feng, J. K.; Ren, A. M.; Zhang, M.; Ma, Y. G.; Liu, X. D. *Eur. J. Inorg. Chem.* **2005**, 1867−1879.
(46) Costa, R. D.; Tordera, D.; Ortí, E.; Bolink, H. J.; Schönle, J.; Graber, S.; Housecroft, C. E.; Constable, E. C.; Zampese, J. A. *J. Mater. Chem.* **2011**, *21*, 16108−16118.
(47) Saito, K.; Arai, T.; Takahashi, N.; Tsukuda, T.; Tsubomura, T. *Dalton Trans.* **2006**, 4444−4448.
(48) (a) Vorontsov, I. I.; Graber, T.; Kovalevsky, A. Y.; Novozhilova, I. V.; Gembicky, M.; Chen, Y.-S.; Coppens, P. *J. Am. Chem. Soc.* **2009**, *131*, 6566−6573. (b) Iwamura, M.; Watanabe, H.; Ishii, K.; Takeuchi, S.; Tahara, T. *J. Am. Chem. Soc.* **2011**, *133*, 7728−7736. (c) Siddique, Z. A.; Yamamoto, Y.; Ohno, T.; Nozaki, K. *Inorg. Chem.* **2003**, *42*, 6366−6378.
(49) (a) McCormick, T.; Jia, W.-L.; Wang, S. *Inorg. Chem.* **2006**, *45*, 147−155. (b) Sakaki, S.; Mizutani, H.; Kase, Y.-I.; Inokuchi, K.-J.; Arai, T.; Hamada, T. *J. Chem. Soc., Dalton Trans.* **1996**, 1909−1914.
(50) (a) Everly, R. M.; Ziessel, R.; Suffert, J.; McMillin, D. R. *Inorg. Chem.* **1991**, *30*, 559−561. (b) Cunningham, C. T.; Cunningham, K. L. H.; Michalec, J. F.; McMillin, D. R. *Inorg. Chem.* **1999**, *38*, 4388−4392. (c) Del Paggio, A. A.; McMillin, D. R. *Inorg. Chem.* **1983**, *22*, 691−692.
(51) Kovalevsky, A. Y.; Gembicky, M.; Novozhilova, I. V.; Coppens, P. *Inorg. Chem.* **2003**, *42*, 8794−8802.
(52) Cunningham, C. T.; Moore, J. J.; Cunningham, K. L. H.; Fanwick, P. E.; McMillin, D. R. *Inorg. Chem.* **2000**, *39*, 3638−3644.
(53) Nomoto, K.; Kume, S.; Nishihara, H. *J. Am. Chem. Soc.* **2009**, *131*, 3830−3831.
(54) Kume, S.; Nomoto, K.; Kusamoto, T.; Nishihara, H. *J. Am. Chem. Soc.* **2009**, *131*, 14198−14199.
(55) Kume, S.; Nishihara, H. *Chem. Commun.* **2011**, *47*, 415−417.
(56) Kume, S.; Nishihara, H. *Dalton Trans.* **2011**, *40*, 2299−2305.
(57) Nishikawa, M.; Nomoto, K.; Kume, S.; Inoue, K.; Sakai, M.; Fujii, M.; Nishihara, H. *J. Am. Chem. Soc.* **2010**, *132*, 9579−9581.
(58) Nishikawa, M.; Nomoto, K.; Kume, S.; Nishihara, H. *J. Am. Chem. Soc.* **2012**, *134*, 10543−10553.
(59) Example for other types of coordinated ligand rotational isomerization such as those based on the Re−C double bond. McCormick, F. B.; Kiel, W. A.; Gladysz, J. A. *Organometallics* **1982**, *1*, 405−408.
(60) Ruthkosky, M.; Kelly, C. A.; Castellano, F. N.; Meyer, G. J. *Coord. Chem. Rev.* **1998**, *171*, 309−322.
(61) Miller, M. T.; Gantzel, P. K.; Karpishin, T. B. *Inorg. Chem.* **1998**, *37*, 2285−2290.
(62) Rorabacher, D. B. *Chem. Rev.* **2004**, *104*, 651−697.
(63) Le Poul, N.; Campion, M.; Douziech, B.; Rondelez, Y.; Le Clainche, L.; Reinaud, O.; Le Mest, Y. *J. Am. Chem. Soc.* **2007**, *129*, 8801−8810.
(64) Merrill, C. L.; Wilson, L. J.; Thamann, T. J.; Loehr, T. M.; Ferris, N. S.; Woodruff, W. H. *J. Chem. Soc., Dalton Trans.* **1984**, 2207−2221.
(65) Liang, H.-C.; Kim, E.; Incarvito, C. D.; Rheingold, A. L.; Karlin, K. D. *Inorg. Chem.* **2002**, *41*, 2209−2212.
(66) Letko, C. S.; Rauchfuss, T. B.; Zhou, X.; Gray, D. L. *Inorg. Chem.* **2012**, *51*, 4511−4520.
(67) Lee, Y.; Lee, D.-H.; Park, G. Y.; Lucas, H. R.; Narducci Sarjeant, A. A.; Kieber-Emmons, M. T.; Vance, M. A.; Milligan, A. E.; Solomon, E. I.; Karlin, K. D. *Inorg. Chem.* **2010**, *49*, 8873−8885.
(68) Bain, A. D. *Prog. Nucl. Magn. Reson. Spectrosc.* **2003**, *43*, 63−103.
(69) Sandström, J. *Dynamic NMR Spectroscopy*; Academic Press: London, 1982.
(70) (a) Hiraoka, S.; Okuno, E.; Tanaka, T.; Shiro, M.; Shionoya, M. *J. Am. Chem. Soc.* **2008**, *130*, 9089−9098. (b) Hiraoka, S.; Hisanaga, Y.; Shiro, M.; Shionoya, M. *Angew. Chem., Int. Ed.* **2010**, *49*, 1669−1673.
(71) Kilbas, B.; Mirtschin, S.; Scopelliti, R.; Severin, K. *Chem. Sci.* **2012**, *3*, 701−704.
(72) Leigh, D. A.; Morales, M. A. F.; Pérez, E. M.; Wong, J. K. Y.; Saiz, C. G.; Slawin, A. M. Z.; Carmichael, A. J.; Haddleton, D. M.; Brouwer, A. M.; Buma, W. J.; Wurpel, G. W. H.; León, S.; Zerbetto, F. *Angew. Chem., Int. Ed.* **2005**, *44*, 3062−3067.
(73) Gong, C.; Gibson, H. W. *Angew. Chem., Int. Ed. Engl.* **1997**, *36*, 2331−2333.
(74) Wilmes, G. M.; France, M. B.; Lynch, S. R.; Waymouth, R. M. *Organometallics* **2004**, *23*, 2405−2411.
(75) Tafazzoli, M.; Ziyaei-Halimjani, A.; Ghiasi, M.; Fattahi, M.; Saidi, M. R. *J. Mol. Struct.* **2008**, *886*, 24−31.
(76) Gennari, M.; Lanfranchi, M.; Cammi, R.; Pellinghelli, M. A.; Marchiò, L. *Inorg. Chem.* **2007**, *46*, 10143−10152.
(77) Nakafuji, S.; Kobayashi, J.; Kawashima, T.; Schmidt, M. W. *Inorg. Chem.* **2005**, *44*, 6500−6502.
(78) Blom, R.; Swang, O. *Eur. J. Inorg. Chem.* **2002**, 411−415.
(79) LeSuer, R. J.; Geiger, W. E. *Angew. Chem., Int. Ed.* **2000**, *39*, 248−250.
(80) (a) Medwid, J. B.; Paul, R.; Baker, J. S.; Brockman, J. A.; Du, M. T.; Hallett, W. A.; Hanifin, J. W.; Hardy, R. A.; Tarrant, M. E.; Torley, L. W.; Wrenn, S. *J. Med. Chem.* **1990**, *33*, 1230−1241. (b) Lafferty, J. J.; Case, F. H. *J. Org. Chem.* **1967**, *32*, 1591−1596.
(81) Altomare, A.; Cascarano, G.; Giacovazzo, C.; Guagliardi, A.; Burla, M. C.; Polidori, G.; Camalli, M. *J. Appl. Crystallogr.* **1994**, *27*, 435.
(82) Sheldrick, G. M. *Acta Crystallogr.* **2008**, *A64*, 112−122.

(83) Farrugia, L. J. *J. Appl. Crystallogr.* **1999**, *32*, 837−838.
(84) Fulmer, G. R.; Miller, A. J. M.; Sherden, N. H.; Gottlieb, H. E.; Nudelman, A.; Stoltz, B. M.; Bercaw, J. E.; Goldberg, K. I. *Organometallics* **2010**, *29*, 2176−2179.
(85) Suzuki, K.; Kobayashi, A.; Kaneko, S.; Takehira, K.; Yoshihara, T.; Ishida, H.; Shiina, Y.; Oishi, S.; Tobita, S. *Phys. Chem. Chem. Phys.* **2009**, *11*, 9850−9860.
(86) Atkins, P.; De Paula, J. *Physical Chemistry*, 8th ed.; W. H. Freeman: New York, 2006.